

Spatiotemporal Dynamics in a Time-Delayed *Rhizophagus grandis-Dendroctonus valens* Predator-Prey System with Nonlocal Diffusion and Taxis

Bowei Xu, Yuting Ding*

College of Science, Northeast Forestry University, Harbin, China

Email: *yuting840810@163.com

How to cite this paper: Xu, B.W. and Ding, Y.T. (2025) Spatiotemporal Dynamics in a Time-Delayed *Rhizophagus grandis-Dendroctonus valens* Predator-Prey System with Nonlocal Diffusion and Taxis. *Journal of Applied Mathematics and Physics*, **13**, 1818-1833.

<https://doi.org/10.4236/jamp.2025.135102>

Received: April 16, 2025

Accepted: May 25, 2025

Published: May 28, 2025

Copyright © 2025 by author(s) and Scientific Research Publishing Inc.

This work is licensed under the Creative Commons Attribution International License (CC BY 4.0).

<http://creativecommons.org/licenses/by/4.0/>



Open Access

Abstract

The objective of this study is to investigate the spatiotemporal dynamics of a *Rhizophagus grandis-Dendroctonus valens* predator-prey system. Under Neumann boundary conditions, we establish a reaction-diffusion system incorporating Holling-II functional response, nonlocal effect, predator-prey taxis and time delay to elucidate the regulatory mechanisms of chemotactic behaviors and delayed predation pressure on ecosystem stability. In addition, we investigate the existence conditions for Hopf bifurcation and employ the multiple time scales method to derive its normal form. Under appropriate parameter constraints, numerical simulations demonstrate that the system exclusively exhibits Hopf bifurcation in the current parameter configuration, where nonlocal interactions, taxis and time delays synergistically induce the formation of spatially heterogeneous periodic solutions. These results elucidate the intrinsic mechanism underlying periodic pest outbreaks and provide a theoretical foundation for optimizing biological control strategies. Notably, our analysis reveals the critical role of predator taxis capability and delayed predation feedback in stabilizing pest population cycles, offering practical guidance for sustainable forest pest management.

Keywords

Predator-Prey, Hopf Bifurcation, Time Delay, Nonlocal, Taxis

1. Introduction

Dendroctonus valens is a globally distributed forest pest exhibiting significant ecological role divergence across regions. Research has demonstrated that *Den-*

droctonus valens functions as a secondary pest of *Pinus* spp. across its native range spanning the United States, Mexico and Canada, where it typically coexists with competitively dominant bark beetle species [1]. Stand mortality or large-scale outbreaks attributed solely to *Dendroctonus valens* are statistically negligible in native ecosystems, with economic impacts confined to timber industry losses. However, since its initial detection in Jincheng, Shanxi Province, China, the invasive population has undergone a behavioral phase transition, exhibiting exponential spread to adjacent regions including Hebei, Henan, Beijing and other neighboring areas, resulting in a cumulative death toll exceeding 10 million host trees [2]. The current climatically suitable habitats for *Dendroctonus valens* in China are concentrated in southern and northern regions, yet under global warming scenarios, the potential distribution demonstrates a monotonic expansion trend: an outbreak in the Liaoning-Inner Mongolia border region in 2017 confirmed its invasion into northeastern China [3]. The infestation dynamics follow a distinct mechanistic pattern as illustrated in **Figure 1**: adults colonize pine trunks through wounds, oviposit between the phloem, cambium and disrupt vascular transport through feeding, inducing host mortality within a two-year time horizon. This delayed mortality mechanism permits multiple larval cohorts to complete development, while adult dispersal to neighboring healthy trees generates a positive feedback loop sustaining infestation cycles.

Traditional control methods, such as aluminum phosphide fumigation and trunk spraying, are partially effective but risk environmental pollution and harm to beneficial insects. In the context of low-carbon environmental protection, biological control has gained prominence. Early studies in Georgia demonstrated the efficacy of *Rhizophagus grandis* against *Dendroctonus micans*. Yang *et al.* [4] proposed using *Rhizophagus grandis* to control *Dendroctonus valens*. Zhao *et al.* [5] explored Braconidae as supplementary agents to control it. However, predatory natural enemies exhibit superior long-term control due to their host-specificity and adaptability.

Mathematical ecology provides a powerful analytical framework for deciphering predator-prey dynamics. From the Malthusian exponential growth model and Verhulst's resource-limited logistic framework to the Lotka-Volterra system describing interspecific interactions, the development of mathematical models has continued to deepen our understanding of ecological complexity [6]. Modern theoretical advancements incorporating functional response functions, reaction-diffusion systems, and nonlocal effects enable precise characterization of spatial heterogeneity in ecosystems. Holling's experimental derivation of functional responses addresses the omission of predator handling time and conversion efficiency in classical models [7]. Rabia *et al.* [8] revealed bifurcation-chaos dynamics and their ecological implications in discrete Holling-II systems through stability analysis. In the realm of reaction-diffusion systems, PDE outperform ODE in resolving spatial heterogeneity. For example, Du *et al.*'s Lotka-Volterra competition model with nonlocal diffusion and free boundaries, combined with parameter k

analysis, elucidated long-term survival-extinction mechanisms of invasive species during boundary expansion [9]. Víctor *et al.* [10] analyzed the persistence of three species in a three-level food chain model, illustrating that the existence of a zero-Hopf equilibrium occurs exclusively under Holling type III or IV functional responses. Wang's reaction-diffusion model with spatial memory uncovers Turing-Hopf bifurcation mechanisms and complex spatiotemporal patterns driven by the synergy of perceptual scale and memory delay [11]. Song *et al.* [12] confirmed the existence of spatially inhomogeneous periodic solutions and heteroclinic orbits through integrating nonlocal interactions with time delays.

It is crucial to emphasize that when analyzing the behavior of complex dynamical systems, normal form analysis serves as a fundamental methodology, with the center manifold deduction [13]-[15] and the multiple scales method [16] [17] being two primary techniques for deriving normal forms. Ding *et al.* [18] rigorously proved the equivalence between third-order Hopf bifurcation normal forms obtained via MTS and CMR for abstract diffusive equations.

Building upon these theoretical advances, this study investigates *Rhizophagus grandis*-mediated biocontrol of *Dendroctonus valens* through the following structure. In Section 2, we establish a spatiotemporal dynamical model integrating nonlocal competition, prey-taxis behavior and time delay effects. In Section 3, we conduct stability analysis of equilibrium points to derive sufficient conditions for Hopf bifurcation occurrence. In Section 4, we employ the multiple scales method to derive the normal form, thereby revealing critical bifurcation characteristics. In Section 5, we perform numerical simulations under biologically feasible parameter configurations to validate theoretical predictions and provide ecological interpretations. A conclusion is given in Section 6.

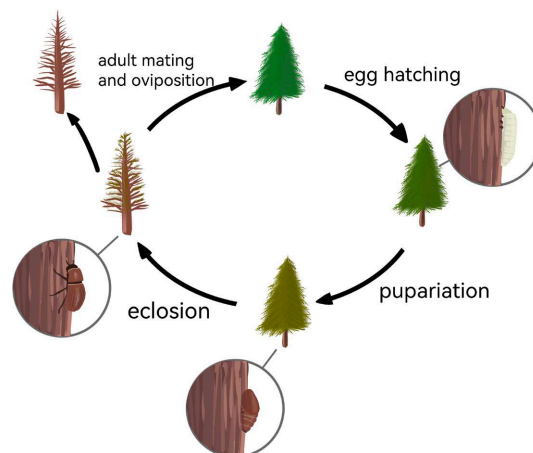


Figure 1. Schematic diagram of *Dendroctonus valens* infesting pine trees.

2. Model Construction

Considering the predation mechanism of the natural enemy *Rhizophagus grandis* on *Dendroctonus valens*, the classical Lotka-Volterra model is formulated as:

$$\begin{cases} \frac{dx}{dt} = x(a - by), \\ \frac{dy}{dt} = y(kx - l), \end{cases} \quad (1)$$

where a , b , k and l are positive constants, y denotes the predator species and x represents its prey.

To reflect the processing time of predators and other factors, we incorporate Holling-II functional responses [19]. Since *Dendroctonus valens* has very strong mobility and it can locate hosts by the smell of their prey's feces and migrate by flying or crawling to find the larvae of *Dendroctonus valens* [4]. Therefore, inspired by [20] [21] [22], we introduce the prey-taxis $-\eta \cdot \nabla(v \nabla u)$ and

$\hat{u} = \int_{\Omega} G(x, y)u(y, t)dy$ into our model, where $G(x, y) = \frac{1}{|\Omega|}$ can be justified

by averaged density in $\Omega = (0, \pi)$.

In this study, we consider the mechanism by which *Rhizophagus grandis* preys on *Dendroctonus valens*. Literature indicates that *Rhizophagus grandis* feeds mainly on the eggs, larvae and pupae of *Dendroctonus valens* [4]. In order to incorporate the time-delayed effect of egg predation behavior on the population decline of *Dendroctonus valens*, we introduce a time delay term into the functional response [23] [24]. Consistent with biocontrol practices, natural enemies are released at pest distribution edges, prompting the use of homogeneous Neumann boundary conditions [5]. The final optimized spatiotemporal model is formulated as:

$$\begin{cases} \frac{\partial u(x, t)}{\partial t} = d_1 \Delta u + ru \left(1 - \frac{\hat{u}}{K}\right) - \frac{\alpha u(x, t - \tau)v(x, t - \tau)}{1 + \alpha u(x, t - \tau)h}, & x \in \Omega, t > 0, \\ \frac{\partial v(x, t)}{\partial t} = d_2 \Delta v - d_3 v + \frac{\beta \alpha u v}{1 + \alpha u h} - \eta \cdot \nabla(v \nabla u), & x \in \Omega, t > 0, \\ \frac{\partial u}{\partial \mathbf{n}} = \frac{\partial v}{\partial \mathbf{n}} = 0, & x \in \partial \Omega, t \geq 0, \\ u(x, t) = \varphi_u \geq 0, v(x, t) = \varphi_v \geq 0, & x \in \Omega, t \in [-\tau, 0], \end{cases} \quad (2)$$

where $u(x, t)$, $v(x, t)$ describe the density of the prey/predator, respectively, at position x and time t , $d_1 > 0$, $d_2 > 0$ are the diffusion coefficients of *Dendroctonus valens* and *Rhizophagus grandis*, respectively, Δ is the Laplacian operator, d_3 is the *Rhizophagus grandis* mortality, r is intrinsic growth rate, K is environmental capacity, h is the time it takes a predator to hunt and process its prey, η is the identification diffusion coefficients of *Rhizophagus grandis*, β is the energy conversion efficiency and \mathbf{n} is the outer normal vector of the boundary $\partial \Omega$.

3. Stability and Bifurcation Analysis

System (2) admits two boundary equilibria $E_0 = (0, 0)$ and $E_1 = (K, 0)$. If the following assumption holds:

$$(H_0) \quad K > \frac{d_3}{\alpha(\beta - d_3 h)} > 0,$$

then system (2) must have a positive constant steady equilibrium $E_* = (u_*, v_*)$, with

$$0 < u_* = \frac{d_3}{\alpha\beta - \alpha d_3 h} < K, \quad v_* = \frac{\beta}{d_3} \left[ru_* \left(1 - \frac{u_*}{K} \right) \right].$$

The linearized system is given as:

$$\begin{aligned} \frac{\partial}{\partial t} \begin{pmatrix} u(x,t) \\ v(x,t) \end{pmatrix} = & J_1 \begin{pmatrix} \Delta u(x,t) \\ \Delta v(x,t) \end{pmatrix} + J_2 \begin{pmatrix} (uv_x)_x \\ (vu_x)_x \end{pmatrix} + J_3 \begin{pmatrix} u(x,t) \\ v(x,t) \end{pmatrix} \\ & + J_4 \begin{pmatrix} \hat{u}(x,t) \\ \hat{v}(x,t) \end{pmatrix} + J_5 \begin{pmatrix} u(x,t-\tau) \\ v(x,t-\tau) \end{pmatrix}, \end{aligned} \tag{3}$$

where

$$\begin{aligned} J_1 = & \begin{pmatrix} d_1 & 0 \\ 0 & d_2 \end{pmatrix}, \quad J_2 = \begin{pmatrix} 0 & 0 \\ -\eta v_* & 0 \end{pmatrix}, \quad J_3 = \begin{pmatrix} a_{11} & 0 \\ a_{21} & 0 \end{pmatrix}, \\ J_4 = & \begin{pmatrix} b_{11} & 0 \\ 0 & 0 \end{pmatrix}, \quad J_5 = \begin{pmatrix} c_{11} & c_{12} \\ 0 & 0 \end{pmatrix}, \end{aligned} \tag{4}$$

with

$$\begin{aligned} a_{11} = & r \left(1 - \frac{u_*}{K} \right), \quad a_{21} = \frac{\beta \alpha v_*}{(1 + \alpha u_* h)^2}, \quad b_{11} = -\frac{ru_*}{K}, \\ c_{11} = & -\frac{\alpha v_*}{(1 + \alpha u_* h)^2}, \quad c_{12} = -\frac{\alpha u_*}{1 + \alpha u_* h}. \end{aligned} \tag{5}$$

Hence, the characteristic system of (2) at $E = (u_*, v_*)$ is given as follows:

$$\lambda^2 + A_n \lambda + B_n + C_n e^{-\lambda \tau} + D_n \lambda e^{-\lambda \tau} = 0, \tag{6}$$

where

$$\begin{cases} A_n = (d_1 + d_2)n^2 - a_{11} - b_{11}\delta_n, \\ B_n = d_1 d_2 n^4 - a_{11} d_2 n^2, \\ C_n = -(c_{12} \eta v_* + c_{11} d_2)n^2 - a_{21} c_{12}, \\ D_n = -c_{11}, \end{cases}$$

with

$$\delta(n) = \begin{cases} 1, & n = 0, \\ 0, & n \in \mathbb{Z}^+. \end{cases}$$

When $\tau = 0$, Equation (6) becomes $\lambda^2 - (A_n + D_n)\lambda + (B_n + C_n) = 0$. For the equilibrium E_* to be locally asymptotically stable, two conditions must simultaneously hold for all $n \in \mathbb{N}$: (i) $A_n + D_n > 0$, (ii) $B_n + C_n > 0$.

For condition (i), we observe that

$A_n + D_n = (d_1 + d_2)n^2 - (a_{11} + c_{11}) > -(a_{11} + c_{11}) > 0$, which directly yields the parameter constraint $K > \frac{d_3(1 + \alpha u_* h)^2}{\beta \alpha^2 h u_* \left(1 - \frac{u_*}{K} \right)}$. Regarding condition (ii),

$g(n) \triangleq B_n + C_n = d_1 d_2 n^4 - (a_{11} d_2 + c_{11} d_2 + c_{12} \eta u_*) n^2 - a_{21} c_{12} > 0$ requires careful

analysis. Let $\zeta = n^2$, we obtain $w(\zeta) = d_1 d_2 \zeta^2 - (a_{11} d_2 + c_{11} d_2 + c_{12} \eta u_*) \zeta - a_{21} c_{12}$. When the discriminant of $w(\zeta)$, denoted as

$\Delta_1 = (a_{11} d_2 + c_{11} d_2 + c_{12} \eta u_*)^2 + 4 d_1 d_2 a_{21} c_{12} < 0$, the inequality automatically holds.

When the discriminant $\Delta_1 \geq 0$, we analyze its symmetry axis given by

$\zeta = \frac{a_{11} d_2 + c_{11} d_2 + c_{12} \eta u_*}{2 d_1 d_2}$. If $\zeta < 0$, that is $\eta > \frac{\alpha d_2 v_* h}{1 + \alpha u_* h}$, since $\zeta = n^2 > 0$, we

can obviously find that the inequality holds for all $n \in \mathbb{N}$. If $\zeta > 0$, that is $\eta < \frac{\alpha d_2 v_* h}{1 + \alpha u_* h}$, we need to meet the following conditions: $g(\lceil \sqrt{\zeta} \rceil) > 0$ and

$g(\lfloor \sqrt{\zeta} \rfloor) > 0$.

In summary, we establish three mutually exclusive stability hypotheses:

$$(H_{11}) \begin{cases} K > \frac{d_3 (1 + \alpha u_* h)^2}{\beta \alpha^2 h u_* \left(1 - \frac{u_*}{K}\right)}, \\ \Delta_1 < 0, \end{cases} \tag{7}$$

$$(H_{12}) \begin{cases} K > \frac{d_3 (1 + \alpha u_* h)^2}{\beta \alpha^2 h u_* \left(1 - \frac{u_*}{K}\right)}, \\ \Delta_1 \geq 0, \\ \eta > \frac{\alpha d_2 v_* h}{1 + \alpha u_* h}, \end{cases} \tag{8}$$

$$(H_{13}) \begin{cases} K > \frac{d_3 (1 + \alpha u_* h)^2}{\beta \alpha^2 h u_* \left(1 - \frac{u_*}{K}\right)}, \\ \Delta_1 \geq 0, \\ \eta < \frac{\alpha d_2 v_* h}{1 + \alpha u_* h}, \\ f(\lceil \sqrt{\zeta} \rceil) > 0, f(\lfloor \sqrt{\zeta} \rfloor) > 0. \end{cases} \tag{9}$$

Considering $\tau > 0$ and substituting $\lambda = \pm i\omega$ ($\omega > 0$) into Equation (6), we separate the real and imaginary parts to obtain the following results:

$$\begin{cases} \cos \omega \tau = \frac{(C_n - A_n D_n) \omega^2 - B_n C_n}{C_n^2 + D_n^2 \omega^2}, \\ \sin \omega \tau = \frac{D_n \omega^3 + (A_n C_n - B_n D_n) \omega}{C_n^2 + D_n^2 \omega^2}, \end{cases} \tag{10}$$

with $n = 0, 1, 2, \dots$.

When both sides of the system are squared and then summed, the following result is obtained:

$$\omega^4 + (A_n^2 - 2B_n - D_n^2) \omega^2 + B_n^2 - C_n^2 = 0. \tag{11}$$

Let $z = \omega^2$, we obtain

$$h(z) \triangleq z^2 + (A_n^2 - 2B_n - D_n^2)z + B_n^2 - C_n^2 = 0, \tag{12}$$

and the discriminant is $\Delta = (A_n^2 - 2B_n - D_n^2)^2 - 4(B_n^2 - C_n^2)$.

Assuming $\Delta \neq 0$, since $h(z) = 0$, we can obtain

$$\begin{cases} \omega_{n,1} = \sqrt{z_{n,1}} = \frac{\sqrt{2}}{2} [D_n^2 + 2B_n - A_n^2 + \sqrt{\Delta}]^{\frac{1}{2}}, \\ \omega_{n,2} = \sqrt{z_{n,2}} = \frac{\sqrt{2}}{2} [D_n^2 + 2B_n - A_n^2 - \sqrt{\Delta}]^{\frac{1}{2}}. \end{cases} \tag{13}$$

Thereby,

$$\tau_n^{(j)} = \begin{cases} \frac{1}{\omega_{n,i}} \left(\arccos \frac{(C_n - A_n D_n) \omega^2 - B_n C_n}{C_n^2 + D_n^2 \omega^2} + 2j\pi \right), \sin \omega \tau > 0, \\ \frac{1}{\omega_{n,i}} \left(2\pi - \arccos \frac{(C_n - A_n D_n) \omega^2 - B_n C_n}{C_n^2 + D_n^2 \omega^2} + 2j\pi \right), \sin \omega \tau < 0, \end{cases} \tag{14}$$

with $j \in \mathbb{N}$, $i = 1, 2$.

Assume that the finite or infinite sets

$$\begin{aligned} I_1 &= \{n \in \mathbb{N} \mid \Delta > 0, B_n - C_n < 0\}, \\ I_2 &= \{n \in \mathbb{N} \mid \Delta > 0, B_n - C_n > 0, A_n^2 - 2B_n - D_n^2 < 0\}, \end{aligned} \tag{15}$$

respectively. Denote

$$\tau_c = \min \{ \tau_* \mid \tau_* = \tau_{n,i}^{(j)}, n \in I_1 \text{ or } n \in I_2 \}. \tag{16}$$

Taking τ as a bifurcation parameter, we have

$$\operatorname{Re} \left[\frac{d\tau}{d\lambda} \Big|_{\lambda = \pm i\omega} \right] = \frac{h'(z_{n,i})}{D_n^2 \omega^2 + C_n^2} \begin{cases} > 0, & h'(z_{n,1}) > 0, \\ < 0, & h'(z_{n,2}) < 0. \end{cases} \tag{17}$$

In summary, we can get the following conclusions.

Theorem 1. Suppose (H_{11}) , (H_{12}) or (H_{13}) holds, for system (2), the following statements hold true.

1) If $I_1 = \emptyset$ and $I_2 = \emptyset$, then the positive constant steady state E_* is asymptotically stable for all $\tau \geq 0$.

2) If $I_1 \neq \emptyset$ and $I_2 = \emptyset$, then Equation (12) has only one positive root $z_{n,1}$ for some $n \in I_1$, which implies that the positive constant steady state E_* is asymptotically stable for $0 < \tau < \tau_c$, unstable for $\tau > \tau_c$ and system (2) undergoes Hopf bifurcation near E_* at $\tau = \tau_c$.

3) If $I_1 = \emptyset$ and $I_2 \neq \emptyset$, then Equation (12) has two positive roots $z_{n,1}$ and $z_{n,2}$ for some $n \in I_2$. Denote that $\tau_{n,1}^{(0)}$ is the smallest time delay corresponding to $n \in I_2$. Then, the positive constant steady state E_* is locally asymptotically stable for $\tau \in (0, \tau_{n,1}^{(0)})$ and there will occur stability switching for system (2). System (2) undergoes Hopf bifurcation near E_* at $\tau = \tau_c$.

4) If $I_1 \neq \emptyset$ and $I_2 \neq \emptyset$, then Equation (12) has three positive roots: the root $z_{n_1,1}$ associated with indices $n_1 \in I_1$ and two additional roots $z_{n_2,1}$, $z_{n_2,2}$ corresponding to indices $n_2 \in I_2$, which implies $\omega_{n_1,1}$ ($n_1 \in I_1$), $\omega_{n_2,1}$ and $\omega_{n_2,2}$

($n_2 \in I_2$). Denote that $\tau_{q,1}^{(0)}$ is the smallest time delay corresponding to q ($q \in I_1$ or $q \in I_2$). Then, the positive constant steady state E_* is locally asymptotically stable for $\tau \in (0, \tau_{q,1}^{(0)})$ and there will occur stability switching for system (2). System (2) undergoes Hopf bifurcation near E_* at $\tau = \tau_c$.

4. Normal Form of Hopf Bifurcation

In this section, we use the MTS to derive the normal form of the Hopf bifurcation for system (2). Suppose that the characteristic system (6) has a pair of pure imaginary roots $\lambda = \pm i\omega$ for $\tau = \tau_c$, then system (2) undergoes n_0 -mode Hopf bifurcation near the equilibrium point E_* , then we derive the normal form of Hopf bifurcation of system (2) by the MTS. We choose time delay τ as a bifurcation parameter, where $\tau = \tau_c + \varepsilon\mu$. The parameter ε is a dimensionless scaling factor and μ is a perturbation parameter, τ_c is given in Equation (16).

Let $\tilde{u}(x, \tau t) = u(x, \tau t) - u_*$, $\tilde{v}(x, \tau t) = v(x, \tau t) - v_*$, we still use $u(x, t)$ and $v(x, t)$ to represent $\tilde{u}(x, \tau t)$ and $\tilde{v}(x, \tau t)$, respectively, we have

$$\begin{cases} \frac{\partial u}{\partial t} = \tau \left\{ d_1 \Delta u + ru \left(1 - \frac{u_*}{K} \right) - \frac{r}{K} (u + u_*) \hat{u} - g_1 u(t-1) - g_2 v(t-1) \right. \\ \left. - g_3 u^2(t-1) - g_4 u(t-1)v(t-1) - f_{111} u^3(t-1) - f_{112} v^3(t-1) \right\}, \\ \frac{\partial v}{\partial t} = \tau \left\{ d_2 \Delta v - d_3 v + \beta [g_1 u + g_2 v + g_3 u^2 + g_4 uv + f_{111} u^3 + f_{112} u^2 v] \right. \\ \left. + \eta v u_{xx} - \eta v_* u_{xx} - \eta v_x u_x \right\}, \end{cases} \quad (18)$$

with

$$\begin{aligned} f_0 &= \frac{\alpha u_* v_*}{1 + \alpha u_* h}, f_1 = \frac{\alpha v_*}{(1 + \alpha u_* h)^2}, f_2 = \frac{\alpha u_*}{1 + \alpha u_* h}, f_{11} = -\frac{\alpha^2 h v_*}{(1 + \alpha u_* h)^3}, \\ f_{12} &= \frac{\alpha}{(1 + \alpha u_* h)^2}, f_{111} = \frac{\alpha^3 h^2 v_*}{(1 + \alpha u_* h)^4}, f_{112} = -\frac{\alpha^2 h}{(1 + \alpha u_* h)^3}, \\ g_1 &= \frac{\alpha v_* (\alpha^2 u_*^2 h^2 + 2)}{(1 + \alpha u_* h)^4}, g_2 = \frac{\alpha u_* (\alpha^2 u_*^2 h^2 + 2\alpha u_* h + 2)}{(1 + \alpha u_* h)^3}, \\ g_3 &= \frac{\alpha^2 v_* h (3\alpha u_* h - 2)}{(1 + \alpha u_* h)^3}, g_4 = \frac{\alpha (1 - \alpha u_* h)}{(1 + \alpha u_* h)^3}. \end{aligned}$$

Let $h = (h_{11}, h_{12})^T$ be the eigenvector corresponding to the eigenvalue $\lambda = i\omega\tau_c$ for the linear operator of Equation (18) and let $h^* = \rho(h_{21}, h_{22})^T$ be the normalized eigenvector corresponding to the eigenvalue $\lambda = -i\omega\tau_c$ for the adjoint operator of the linear operator in Equation (18). According to the condition $\langle \overline{h^*}, h \rangle = 1$, we can proceed with the following analysis:

$$\begin{cases} h = \left(1, \frac{\eta v_* n^2 + a_{21}}{d_2 n^2 + i\omega} \right)^T, \\ h^* = \rho \left(\frac{d_2 n^2 - i\omega}{c_{12} e^{i\omega\tau_c}}, 1 \right)^T, \end{cases} \quad (19)$$

with $\rho = (\overline{h_{11} h_{21}} + h_{22} \overline{h_{12}})^{-1}$.

We assume that the solution of Equation (18) is:

$$Z(x, t) = Z(x, T_0, T_1, T_2, \dots) = \sum_{k=1}^{\infty} \varepsilon^k Z_k(x, T_0, T_1, T_2, \dots), \tag{20}$$

where $T_i = \varepsilon^i t$ ($i = 0, 1, 2, \dots$). The derivation with respect to t is

$$\frac{d}{dt} = \frac{\partial}{\partial T_0} + \varepsilon \frac{\partial}{\partial T_1} + \varepsilon^2 \frac{\partial}{\partial T_2} + \dots = D_0 + \varepsilon D_1 + \varepsilon^2 D_2 + \dots, \tag{21}$$

where the differential operator $D_i = \frac{\partial}{\partial T_i}$ ($i = 0, 1, 2, \dots$). We expand $Z(x, t-1)$ at $Z(x, T_0-1, T_1, T_2, \dots)$, we obtain

$$Z(x, t-1) = \varepsilon Z_{11} + \varepsilon^2 Z_{21} - \varepsilon^2 D_1 Z_{11} + \varepsilon^3 Z_{31} - \varepsilon^3 D_1 Z_{21} - \varepsilon^3 D_2 Z_{11} + \dots, \tag{22}$$

where $Z_{j,1} = Z_j(x, T_0-1, T_1, T_2, \dots)$, $j = 1, 2, 3, \dots$.

Substituting Equations (20)-(22) into Equation (18). For the ε , we obtain

$$\begin{cases} D_0 u_1 - \tau_c \left[d_1 \Delta u_1 + r u_1 \left(1 - \frac{u_*}{K} \right) - \frac{r u_*}{K \pi} \int_0^\pi u_1 dx - g_1 u_{11} - g_2 v_{11} \right] = 0, \\ D_0 v_1 - \tau_c \left[d_2 \Delta v_1 - d_3 v_1 + \beta (g_1 u_1 + g_2 v_1) - \eta v_* u_{1,xx} \right] = 0. \end{cases} \tag{23}$$

The solution of Equation (19) can be written as follows:

$$\begin{cases} u_1 = G e^{i\omega\tau_c T_0} h_{11} \cos(nx) + c.c., \\ v_1 = G e^{i\omega\tau_c T_0} h_{12} \cos(nx) + c.c., \end{cases} \tag{24}$$

where h_{11} and h_{12} are given in Equation (19), $c.c.$ means the complex conjugate of the preceding terms.

For the ε^2 , we have

$$\begin{cases} D_0 u_2 - \tau_c \left[d_1 \Delta u_2 + r u_2 \left(1 - \frac{u_*}{K} \right) - \frac{r u_*}{K \pi} \int_0^\pi u_2 dx \right] + g_1 u_{21} + g_2 v_{21} \\ = -D_1 u_1 + \tau_c \left[-\frac{r u_1}{K \pi} \int_0^\pi u_1 dx + g_1 D_1 u_{11} + g_2 D_1 v_{11} - g_3 u_{11}^2 - g_4 u_{11} v_{11} \right] \\ + \mu \left[d_1 \Delta u_1 + r u_1 \left(1 - \frac{u_*}{K} \right) - \frac{r u_*}{K \pi} \int_0^\pi u_1 dx - g_1 u_{11} - g_2 v_{11} \right], \\ D_0 v_2 - \tau_c \left[d_2 \Delta v_2 - d_3 v_2 + \beta (g_1 u_2 + g_2 v_2) - \eta v_* u_{2,xx} \right] \\ = -D_1 v_1 + \tau_c \left[\beta (g_3 u_1^2 + g_4 u_1 v_1) - \eta v_1 u_{1,xx} - \eta u_{1,x} v_{1,x} \right] \\ + \mu \left[d_2 \Delta v_1 - d_3 v_1 + \beta (g_1 u_1 + g_2 v_1) - \eta v_* u_{1,xx} \right]. \end{cases} \tag{25}$$

Substituting Equation (24) into Equation (25), by solvability condition, we obtain

$$\frac{\partial G}{\partial T_1} = \mu M G, \tag{26}$$

with

$$\begin{cases} M = \frac{\overline{\rho h_{21}} \ell_1 + \overline{\rho h_{22}} \ell_2}{\rho h_{22} h_{21} - \overline{\rho h_{21}} \left[\tau_c e^{-i\omega\tau_c} (g_1 h_{11} + g_2 h_{12}) - h_{11} \right]}, \\ \ell_1 = -d_1 n_0^2 h_{11} + r h_{11} \left(1 - \frac{u_*}{K} \right) - g_1 h_{11} e^{-i\omega\tau_c} - g_2 h_{12} e^{-i\omega\tau_c}, \\ \ell_2 = -d_2 n_0^2 h_{12} - d_3 h_{12} + \eta v_* n_0^2 h_{11}. \end{cases}$$

Assume the solution of Equation (25) to be as follows:

$$\begin{cases} u_2 = \sum_{k=0}^{+\infty} (j_{0k} G\bar{G} + j_{1k} e^{2i\omega t_0} G^2 + \bar{j}_{1k} e^{-2i\omega t_0} \bar{G}^2) \cos(kx), \\ v_2 = \sum_{k=0}^{+\infty} (p_{0k} G\bar{G} + p_{1k} e^{2i\omega t_0} G^2 + \bar{p}_{1k} e^{-2i\omega t_0} \bar{G}^2) \cos(kx). \end{cases} \quad (27)$$

Substituting solutions Equation (24) and Equation (27) into Equation (25), we obtain

$$\begin{aligned} j_{0k} &= \frac{Ay_2 - By_1}{x_1 y_2 - x_2 y_1}, & j_{1k} &= \frac{Cy_4 - Dy_3}{x_3 y_4 - x_4 y_3}, \\ p_{0k} &= \frac{Ax_2 - Bx_1}{y_1 x_2 - y_2 x_1}, & p_{1k} &= \frac{Cx_4 - Dx_3}{y_3 x_4 - y_4 x_3}, \end{aligned} \quad (28)$$

where

$$\begin{cases} A = \frac{2r}{K\pi} h_{11} \bar{h}_{11} \psi_K \int_0^\pi \cos(n_0 x) dx + [2g_3 h_{11} \bar{h}_{11} + g_4 (h_{11} \bar{h}_{12} + h_{12} \bar{h}_{11})] \theta_K, \\ B = -[2g_3 \beta h_{11} \bar{h}_{11} + g_4 \beta (h_{11} \bar{h}_{12} + h_{12} \bar{h}_{11}) + \eta n_0^2 (h_{11} \bar{h}_{12} + h_{12} \bar{h}_{11})] \theta_K \\ \quad - \eta n_0^2 (h_{11} \bar{h}_{12} + h_{12} \bar{h}_{11}) \phi_K, \\ C = -\frac{r h_{11}^2}{K\pi} \psi_K \int_0^\pi \cos(n_0 x) dx - [(g_3 h_{11}^2 + g_4 h_{11} h_{12}) e^{-2i\omega \tau_c}] \theta_K, \\ D = (g_3 \beta h_{11}^2 + g_4 \beta h_{11} h_{12} + \eta n_0^2 h_{11} h_{12}) \theta_K - \eta n_0^2 h_{11} h_{12} \phi_K, \\ x_1 = -\sum_{k=0}^{+\infty} \left\{ \left[d_1 k^2 + r \left(1 - \frac{u_*}{K} \right) - g_1 \right] \int_0^\pi \cos^2(kx) dx + \frac{r u_*}{K\pi} \left(\int_0^\pi \cos(kx) dx \right)^2 \right\}, \\ x_2 = \sum_{k=0}^{+\infty} (\beta g_1 + \eta v_* k^2) \int_0^\pi \cos^2(kx) dx, \\ x_3 = \sum_{k=0}^{+\infty} \left\{ \left[2i\omega + d_1 k^2 + r \left(1 - \frac{u_*}{K} \right) - g_1 e^{-2i\omega \tau_c} \right] \int_0^\pi \cos^2(kx) dx \right. \\ \quad \left. + \frac{r u_*}{K\pi} \left(\int_0^\pi \cos(kx) dx \right)^2 \right\}, \\ x_4 = -\sum_{k=0}^{+\infty} (\beta g_1 + \eta v_* k^2) \int_0^\pi \cos^2(kx) dx, \\ y_1 = g_2 \sum_{k=0}^{+\infty} \int_0^\pi \cos^2(kx) dx, \\ y_2 = -\sum_{k=0}^{+\infty} (d_2 k^2 + d_3 - g_2 \beta) \int_0^\pi \cos^2(kx) dx, \\ y_3 = -g_2 e^{-2i\omega \tau_c} \sum_{k=0}^{+\infty} \int_0^\pi \cos^2(kx) dx, \\ y_4 = \sum_{k=0}^{+\infty} (2i\omega + d_2 k^2 + d_3 - g_2 \beta) \int_0^\pi \cos^2(kx) dx, \end{cases}$$

with

$$\theta_K = \sum_{k=0}^{\infty} \int_0^\pi \cos^2(n_0 x) \cos(kx) dx = \begin{cases} \frac{\pi}{2}, & k = 0, \\ \frac{\pi}{4}, & k = 2n_0, \\ 0, & k \neq 0, 2n_0, \end{cases}$$

$$\phi_K = \sum_{k=0}^{\infty} \int_0^{\pi} \sin^2(n_0x) \cos(kx) dx = \begin{cases} \frac{\pi}{2}, & k = 0, \\ -\frac{\pi}{4}, & k = 2n_0, \\ 0, & k \neq 0, 2n_0, \end{cases}$$

$$\psi_K = \sum_{k=0}^{\infty} \int_0^{\pi} \cos(n_0x) \cos(kx) dx = \begin{cases} \frac{\pi}{2}, & k = n_0, \\ 0, & k \neq n_0. \end{cases}$$

For the ε^3 , we obtain

$$\left\{ \begin{aligned} & D_0 u_3 - \tau_c \left[d_1 \Delta u_3 + r u_3 \left(1 - \frac{u_*}{K} \right) - \frac{r u_*}{K \pi} \int_0^{\pi} u_3 dx + g_1 u_{31} + g_2 v_{31} \right] \\ & = -D_1 u_2 - D_2 u_1 + \tau_c \left[-\frac{r u_1}{K \pi} \int_0^{\pi} u_2 dx - \frac{r u_2}{K \pi} \int_0^{\pi} u_1 dx + g_1 D_1 u_{21} \right. \\ & \quad + g_1 D_2 u_{11} + g_2 D_1 v_{21} + g_2 D_2 v_{11} + 2g_3 u_{11} u_{21} - 2g_3 D_1 u_{11}^2 \\ & \quad \left. + g_4 (2D_1 u_{11} v_{11} - u_{11} v_{21} - u_{21} v_{11}) - f_{111} u_{11}^3 - f_{112} u_{11}^2 v_{11} \right] + o(\mu), \\ & D_0 v_3 - \tau_c \left[d_2 \Delta v_3 - d_3 v_3 + \beta (g_1 u_3 + g_2 v_3) - \eta v_* u_{3,xx} \right] \\ & = -D_1 v_2 - D_2 v_1 + \tau_c \left[\beta (2g_3 u_1 u_2 + g_4 u_1 v_2 + g_4 u_2 v_1 + f_{111} u_1^3 + f_{112} u_1^2 v_1) \right. \\ & \quad \left. - \eta (v_2 u_{1,xx} + v_1 u_{2,xx} + u_{1,x} v_{2,x} + u_{2,x} v_{1,x}) \right] + o(\mu). \end{aligned} \right. \tag{29}$$

Substituting Equation (24) and Equation (27) into Equation (29), by solvability condition, we obtain

$$\frac{\partial G}{\partial T_2} = \frac{HG^2 \bar{G}}{\rho \overline{h_{22} h_{21}} - \overline{\rho h_{21}} \left[\tau_c e^{-i\omega \tau_c} (g_1 h_{11} + g_2 h_{12}) - h_{11} \right] \int_0^{\pi} \cos^2(n_0x) dx}, \tag{30}$$

where

$$\begin{aligned} H = & \tau_c \bar{\rho} \sum_{k=0}^{+\infty} \left\{ \overline{h_{21}} \left[-\frac{r h_{11}}{K \pi} j_{0k} \int_0^{\pi} \cos^2(n_0x) dx \int_0^{\pi} \cos(kx) dx - \frac{r h_{11}}{K \pi} \theta_K \right. \right. \\ & + e^{-i\omega \tau_c T_0} (2g_3 h_{11} j_{0k} - g_4 h_{11} p_{0k} - g_4 h_{12} j_{0k}) \theta_K \\ & \left. \left. - e^{-3i\omega \tau_c T_0} (f_{111} h_{11}^2 \overline{h_{11}} + f_{112} h_{11}^2 h_{12} + 2f_{112} \overline{h_{11}} h_{11} h_{12}) \int_0^{\pi} \cos^4(n_0x) dx \right] \right. \\ & + \overline{h_{22}} \left[(2g_3 h_{11} j_{0k} + g_4 h_{11} p_{0k} + g_4 h_{12} j_{0k}) \theta_K \right. \\ & + (f_{111} h_{11}^2 \overline{h_{11}} + f_{112} h_{11}^2 h_{12} + 2f_{112} \overline{h_{11}} h_{11} h_{12}) \int_0^{\pi} \cos^4(n_0x) dx \\ & + \eta (n_0^2 h_{11} p_{0k} \theta_K + k^2 h_{12} j_{0k} \theta_K - k n_0 h_{11} p_{0k} \int_0^{\pi} \sin(n_0x) \cos(n_0x) \sin(kx) dx \\ & \left. \left. - k n_0 h_{12} j_{0k} \int_0^{\pi} \sin(n_0x) \cos(n_0x) \sin(kx) dx \right] \right\}, \end{aligned}$$

with

$$\int_0^{\pi} \sin(n_0x) \cos(n_0x) \sin(kx) dx = \begin{cases} \frac{\pi}{4}, & k = n_0 + 1, \\ 0, & k \neq n_0 + 1. \end{cases}$$

Therefore, the third-order truncated normal form near the Hopf bifurcation point for system (2) reduced on the center manifold is given by

$$\frac{\partial G}{\partial t} = \mu MG + \frac{HG^2\bar{G}}{\rho h_{22}h_{21} - \overline{\rho h_{21}} \left[\tau_c e^{-i\omega\tau_c} (g_1 h_{11} + g_2 h_{12}) - h_{11} \right] \int_0^\pi \cos^2(n_0 x) dx}, \quad (31)$$

where M and H are defined by Equation (26) and Equation (30).

Let $G = re^{i\theta}$, the normal form near the Hopf bifurcation of system (2) in polar coordinates is written as:

$$\begin{cases} \dot{r} = \text{Re}(M_1)\mu r + \text{Re}(M_2)r^3, \\ \dot{\theta} = \text{Im}(M_1)\mu + \text{Im}(M_2)r^2. \end{cases} \quad (32)$$

Therefore, we have the following theorem.

Theorem 2. For Equation (32), if $\frac{\text{Re}(M_1)\mu}{\text{Re}(M_2)} < 0$ holds, then Equation (32)

has one equilibrium r_* , and there exist bifurcating periodic solutions near the positive constant steady state E_* of system (2). Moreover:

- 1) if $\text{Re}(M_1)\mu < 0$, the bifurcating periodic solutions are unstable, and the direction of bifurcation is forward (backward) for $\mu > 0$ ($\mu < 0$);
- 2) if $\text{Re}(M_1)\mu > 0$, the bifurcating periodic solutions are stable, and the direction of bifurcation is forward (backward) for $\mu > 0$ ($\mu < 0$).

5. Numerical Simulations

In this section, we perform numerical simulations to verify the correctness of the theoretical analysis. Due to the limited availability of actual ecological data, the parameters in this study are established based on the theoretical framework of the system and biological plausibility. Under the constraints that α and h must remain non-zero as established in previous conditions, we implement the following reformulation of the functional response function: $\frac{\alpha uv}{1 + \alpha uh} = \frac{kuv}{D_1 + u}$, where

$D_1 = \frac{1}{\alpha h}$ is the half-saturation constant and $k = \frac{1}{h}$ is a constant.

We provide the following parameters: $d_1 = 0.2$, $d_2 = 0.01$, $d_3 = 0.01$, $D_1 = 9$, $k = 0.2$, $\eta = 1$, $\beta = 1$, $r = 0.2$, $K = 5$ and $l = 1$. Based on the data above, (H₀) always holds, system (2) has two boundary equilibria $E_0 = (0, 0)$, $E_1 = (5, 0)$ and one nontrivial equilibrium $E_* = (u_*, v_*) = (0.4737, 8.5762)$. As mentioned earlier, what we ultimately focus on is nothing but the stability of the nontrivial equilibrium E_* .

When $\tau = 0$ holds, E_* is local asymptotically stable. This means that: although *Dendroctonus valens* and *Rhizophagus grandis* can coexist at this time, natural predators are capable of suppressing the reproduction of the pests.

When $\tau > 0$ holds, (H₁₁) holds for $n = 1$, there does not exist any n such that (H₁₂) and (H₁₃) holds. At this time, we can get the critical delay $\tau_1^{(0)} = 2.0075$. From the definition of τ_c , we obtain $\tau_c = 2.0075$, Theorem 1 supports the conclusion that the positive constant steady state E_* achieves local asymptotic sta-

bility when $\tau \in [0, 2.0075)$ and instability when $\tau \in [2.0075, +\infty)$. We will select appropriate parameter values within the aforementioned regions (stable and unstable states), provide numerical simulation results and rigorously analyze them to validate the theoretical assertions established above. We choose $\tau = 1.75 \in [0, 2.0075)$ and get **Figure 2**.

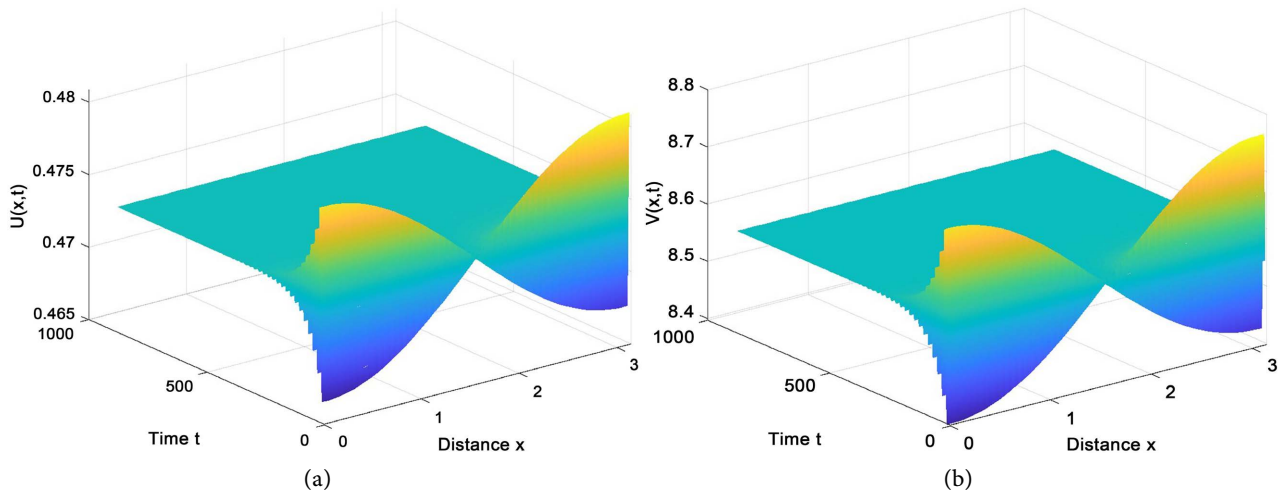


Figure 2. When $\tau = 1.75$, the simulation of system (2) reveals that the equilibrium E_* is locally asymptotically stable.

Then, we choose $\tau = 2.0095$, from Equation (26) and Equation (30), we obtain $\text{Re}(M_1) > 0$, $\text{Re}(M_2) < 0$. Thus, according to Theorem 2, the Equation (2) will generate inhomogeneous periodic solutions near the positive constant steady state E_* of system (2) and bifurcating periodic solutions are stable and forward, as shown in **Figure 3**.

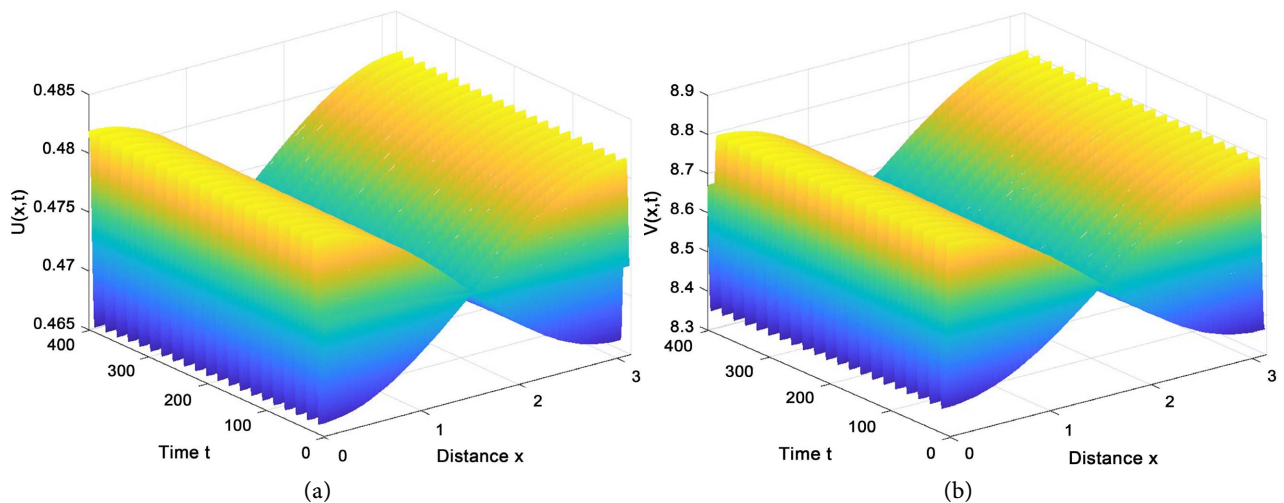


Figure 3. When $\tau = 2.0095$, system (2) produces stable, inhomogeneous forward periodic solutions near E_* .

By analyzing **Figure 2** and **Figure 3**, we can draw the following conclusions.

- 1) As illustrated in **Figure 2**, when the time delay is below the critical threshold,

Rhizophagus grandis can rapidly suppress *Dendroctonus valens* populations to a stable safety level, demonstrating the spatiotemporal controllability of this bio-control strategy.

2) As illustrated in **Figure 3**, when the time delay slightly exceeds the critical threshold, *Rhizophagus grandis* maintains partial control over *Dendroctonus valens* populations, but induces periodic outbreak cycles in the pest population while exhibiting synchronous periodic fluctuations in the predator population.

6. Conclusions

In this study, we established a predator-prey system incorporating nonlocal diffusion, prey-taxis and time delay effects to investigate the spatiotemporal dynamics between *Dendroctonus valens* and its natural enemy *Rhizophagus grandis*. Our theoretical analysis and numerical simulations yielded the following key findings:

When time delay is absent ($\tau = 0$) or below the critical threshold ($\tau < \tau_c$), the positive equilibrium E_* exhibits local asymptotic stability, indicating effective pest suppression by the natural enemy. However, when $\tau \geq \tau_c$, the system undergoes a Hopf bifurcation, generating spatially stable periodic solutions that correspond to cyclical pest outbreaks and predator-prey oscillations. Numerical simulations confirmed the bifurcation behavior at $\tau_c = 2.0095$, validating our theoretical predictions.

From an application perspective, the critical delay τ_c provides important guidance for optimizing the timing of natural enemy releases to prevent system destabilization caused by excessive delays. Enhancing the prey-taxis capability of natural enemies can improve their pest localization efficiency and help suppress periodic outbreaks.

It should be noted that, our model still has certain limitations. Environmental factors such as temperature variations and terrain heterogeneity were not incorporated, which may affect prediction accuracy. Moreover, field population dynamics data for *Dendroctonus valens* and *Rhizophagus grandis* remain scarce. Therefore, all parameters were derived through theoretical analysis.

In our future work, we will collaborate with ecological research teams to systematically enhance both the practical applicability and theoretical rigor of the proposed model. Through comprehensive analysis of the current framework, we intend to identify critical components exerting dominant influences on dynamic properties, subsequently developing simplified yet operationally viable models tailored for practical implementation. These refined models will be rigorously integrated with experimental datasets to establish empirical validation of their real-world predictive capabilities, thereby bridging the gap between theoretical constructs and ecological applications while maintaining methodological coherence across scales.

Acknowledgements

This study was funded by the Heilongjiang Provincial Natural Science Foundation

of China (Grant No. LH2024A001), and the College Students Innovations Special Project funded by Northeast Forestry University (No. DCLXY-2025010).

Conflicts of Interest

The authors declare no conflicts of interest regarding the publication of this paper.

References

- [1] Rappaport, N.G., Owen, D.R. and Stein, J.D. (2001) Interruption of Semiochemical-Mediated Attraction of *Dendroctonus valens* (Coleoptera: Scolytidae) and Selected Nontarget Insects by Verbenone. *Environmental Entomology*, **30**, 837-841. <https://doi.org/10.1603/0046-225x-30.5.837>
- [2] Lv, Q., Zhang, S.F., Lin, R.Z. and Wang, H.M. (2022) Occurrence Status of Main Forestry Invasive Species in China and Their Research Trends. *Plant Protection*, **48**, 21-38. <https://doi.org/10.16688/j.zwbh.2022262>
- [3] Wu, H., Li, D., Luo, Z., He, S., Jiang, S. and Song, Y. (2022) Disaster Risk Analysis of *Dendroctonus valens* in Northeast China. *Forest Pest and Disease*, **41**, 22-28. <https://doi.org/10.19688/j.cnki.issn1671-0886.20220018>
- [4] Zhao, J.X., Yang, Z.Q., Ren, X.H. and Liang, X.M. (2008) Biological Characteristics and Occurring Law of *Dendroctonus valens* in China. *Scientia Silvae Sinicae*, **44**, 99-105.
- [5] Zhao, J.X., Yang, Z.Q. and Liang, Y.J. (2008) Research Advance on Biological Control of Conifer Bark Beetles with the Predator, *Rhizophagus grandis* (Coleoptera: Rhizophagidae). *Scientia Silvae Sinicae*, **44**, 151-156.
- [6] Volterra, V. (1926) Fluctuations in the Abundance of a Species Considered Mathematically1. *Nature*, **118**, 558-560. <https://doi.org/10.1038/118558a0>
- [7] Holling, C.S. (1965) The Functional Response of Predators to Prey Density and Its Role in Mimicry and Population Regulation. *Memoirs of the Entomological Society of Canada*, **97**, 5-60. <https://doi.org/10.4039/entm9745fv>
- [8] Mehdi, R., Wu, R. and Hammouch, Z. (2025) Chaotic Bifurcation Dynamics in Predator-Prey Interactions with Logistic Growth and Holling Type-II Response. *Alexandria Engineering Journal*, **115**, 119-130. <https://doi.org/10.1016/j.aej.2024.11.077>
- [9] Du, Y., Ni, W. and Shi, L. (2025) Long-Time Dynamics of a Competition Model with Nonlocal Diffusion and Free Boundaries: Vanishing and Spreading of the Invader. *SIAM Journal on Mathematical Analysis*, **57**, 1195-1226. <https://doi.org/10.1137/24m1647473>
- [10] Castellanos, V. and Llibre, J. (2025) Persistence and Zero-Hopf Equilibrium in the Tritrophic Food Chain Model with Holling Functional Response. *Nonlinear Analysis: Real World Applications*, **82**, Article 104232. <https://doi.org/10.1016/j.nonrwa.2024.104232>
- [11] Xue, S., Song, Y. and Wang, H. (2024) Spatio-Temporal Dynamics in a Reaction-Diffusion Equation with Nonlocal Spatial Memory. *SIAM Journal on Applied Dynamical Systems*, **23**, 641-667. <https://doi.org/10.1137/22m1543860>
- [12] Song, Y. and Yang, G. (2020) Spatio-Temporal Dynamics of a Reaction-Diffusion Equation with the Nonlocal Spatial Average and Delay. *Applied Mathematics Letters*, **107**, Article 106388. <https://doi.org/10.1016/j.aml.2020.106388>
- [13] Faria, T. and Magalhaes, L.T. (1995) Normal Forms for Retarded Functional Differential Equations with Parameters and Applications to Hopf Bifurcation. *Journal of*

- Differential Equations*, **122**, 181-200. <https://doi.org/10.1006/jdeq.1995.1144>
- [14] Faria, T. (2000) Normal Forms and Hopf Bifurcation for Partial Differential Equations with Delays. *Transactions of the American Mathematical Society*, **352**, 2217-2238. <https://doi.org/10.1090/s0002-9947-00-02280-7>
- [15] Song, Y., Peng, Y. and Zhang, T. (2021) The Spatially Inhomogeneous Hopf Bifurcation Induced by Memory Delay in a Memory-Based Diffusion System. *Journal of Differential Equations*, **300**, 597-624. <https://doi.org/10.1016/j.jde.2021.08.010>
- [16] Nayfeh, A.H. (2007) Order Reduction of Retarded Nonlinear Systems—The Method of Multiple Scales versus Center-Manifold Reduction. *Nonlinear Dynamics*, **51**, 483-500. <https://doi.org/10.1007/s11071-007-9237-y>
- [17] Paquin-Lefebvre, F., Nagata, W. and Ward, M.J. (2019) Pattern Formation and Oscillatory Dynamics in a Two-Dimensional Coupled Bulk-Surface Reaction-Diffusion System. *SIAM Journal on Applied Dynamical Systems*, **18**, 1334-1390. <https://doi.org/10.1137/18m1213737>
- [18] Ding, Y., Liu, G. and Zheng, L. (2023) Equivalence of MTS and CMR Methods Associated with the Normal Form of Hopf Bifurcation for Delayed Reaction-Diffusion Equations. *Communications in Nonlinear Science and Numerical Simulation*, **117**, Article 106976. <https://doi.org/10.1016/j.cnsns.2022.106976>
- [19] Mehdi, R., Wu, R. and Hammouch, Z. (2025) Chaotic Bifurcation Dynamics in Predator-Prey Interactions with Logistic Growth and Holling Type-II Response. *Alexandria Engineering Journal*, **115**, 119-130. <https://doi.org/10.1016/j.aej.2024.11.077>
- [20] Furter, J. and Grinfeld, M. (1989) Local vs. Non-Local Interactions in Population Dynamics. *Journal of Mathematical Biology*, **27**, 65-80. <https://doi.org/10.1007/bf00276081>
- [21] Wang, J., Wu, S. and Shi, J. (2021) Pattern Formation in Diffusive Predator-Prey Systems with Predator-Taxis and Prey-Taxis. *Discrete & Continuous Dynamical Systems B*, **26**, 1273-1289. <https://doi.org/10.3934/dcdsb.2020162>
- [22] Peng, Y. and Zhang, G. (2020) Dynamics Analysis of a Predator-Prey Model with Herd Behavior and Nonlocal Prey Competition. *Mathematics and Computers in Simulation*, **170**, 366-378. <https://doi.org/10.1016/j.matcom.2019.11.012>
- [23] Dubey, B. and Kumar, A. (2019) Dynamics of Prey-Predator Model with Stage Structure in Prey Including Maturation and Gestation Delays. *Nonlinear Dynamics*, **96**, 2653-2679. <https://doi.org/10.1007/s11071-019-04951-5>
- [24] Wang, Y., Shao, Y. and Chai, C. (2023) Dynamics of a Predator-Prey Model with Fear Effects and Gestation Delays. *AIMS Mathematics*, **8**, 7535-7559. <https://doi.org/10.3934/math.2023378>